Hill, I.A., Taira, A., Firth, J.V., et al., 1993
Proceedings of the Ocean Drilling Program, Scientific Results, Vol. 131

23. IN-SITU STRESS CONDITIONS AT NANKAI TROUGH, SITE 808[1]

K. Moran,[2] W. Brückmann,[3] V. Feeser,[4] and R.G. Campanella[5]

ABSTRACT

Shipboard laboratory index property data, shore-based consolidation tests, and in-situ stress and pore-pressure measurements are used in this study to constrain the stress conditions at ODP Site 808, Nankai Trough. Results of these tests are presented along with additional interpretations of porosity rebound and permeability. The sediment at Site 808 is highly affected by excess fluid pressures throughout the sediment column. Excess fluid pressure is severe below the major fault boundary, the décollement. The in-situ measurement of lateral stresses, which are shallow in the sediment section, confirms that the principal stress direction is rotated from a "normal" basin-type condition where the principal stress direction is vertical.

INTRODUCTION

Nankai Trough is one of the best examples of a modern clastic accretionary prism. This region has seen extensive study, including many seismic surveys (e.g., Kaiko I Research Group, 1986) and three drilling cruises, DSDP Leg 31, DSDP Leg 87, and ODP Leg 131 (Fig. 1). Recent studies on modern active margins have suggested that deformation and accretion of sediment at active margins are largely controlled by pore-fluid pressure and fluid flow (Langseth and Moore, 1990). Consequently, the most recent drilling at Nankai Trough emphasized the study of fluids as part of the deformation process at the toe of the accretionary prism. The primary objectives of ODP Leg 131 at Nankai were to investigate the in-situ stresses and fluid pressures, structural geology, physical properties, and pore-water geochemistry of sediments. In addition to the direct application of understanding active margin processes, the results from these studies at modern accretionary complexes can assist in the study of other geologic settings. For example, seismic reflection data from the Nankai Trough region show many features that are characteristics of fold-and-thrust belts: imbricate thrust faults, a well-defined décollement, and fault-bend folds (Moore and Lundberg, 1986).

The studies undertaken during Leg 131 are required for definition of sediment and pore-water characteristics that are the result of the initial deformation process. To complete the story of accretion, however, a knowledge of the effective stress conditions that produce these characteristics is required. Stress conditions at active margins are known to vary significantly from those in basinal-type settings. The wedge morphology resulting from offscraped sediment at active margins suggests high lateral effective stresses (rotation of principal stresses) in these settings. The rotation of principal stresses and pore fluid pressure are two important factors that control the sediment deformation processes in wedge formation and the movement of fluids within these complexes. In addition, there is evidence for high pore-pressures within sediment wedges at other modern accretionary prisms, for example the Lesser Antilles Forearc (Bangs et al., 1990).

This study uses the results from shipboard physical property measurements, one-dimensional consolidation tests, in-situ pore-pressure measurements, and in-situ lateral stress to constrain the effective stress conditions at Site 808. ODP Leg 131 provided the first data set that combines shipboard and shore-based laboratory data with in-situ pressure and stress measurements at a modern accretionary complex, a major achievement in the study of fluid and deformation processes.

METHODS

Laboratory Procedures

Two types of laboratory data are used in this study. The primary data set is the shipboard index property data, specifically bulk density and porosity, measured on recovered core material. Porosity was determined from the direct measurement of bulk density and water content (Shipboard Scientific Party, 1991a). It is well known that the porosity depth or bulk density depth function reflects both the lithology and the stress history of the sediment package. Within the same lithologic unit, the porosity-depth function represents the sediment response to its stress history. A normally consolidated porosity-depth function in sedimentary systems is typically log-linear (Athy, 1930; Terzaghi, 1943). However, the parameters used in these functions are themselves a function of sediment type. Fine-grained normally consolidated pelagic sediment will have higher porosity than coarser clastic sediment at an equivalent depth below seafloor (Brückmann, 1989). Consequently, the porosity-depth function alone can only be used to assess the relative consolidation history, e.g., comparison of porosity values between similar lithologic units can be used to determine which unit is more consolidated.

To provide an absolute assessment of stress history, a second type of laboratory test was used. One-dimensional consolidation tests were run on selected lithologies of Site 808. Casagrande (1932) introduced the concept of normally and overconsolidated soil that is directly applicable to marine sediment. With laboratory one-dimensional consolidation data, sediment can be assessed for its absolute stress history, if it has not been significantly altered by other mechanisms, such as diagenetic processes or sampling disturbance. In this study, selected lithologic units were sampled for shore-based one-dimensional consolidation tests. Tests were run in back-pressured consolidometers (Lowe, 1974) following standard incremental loading procedures (e.g., Holtz and Kovacs, 1981). A load increment ratio of one was used and the samples were back-pressured to 300 kPa to drive any gases into solution prior to the the start of loading.

Downhole Procedures

In-situ lateral stress and pore-pressure measurements were made using a newly designed lateral stress tool, LAST-I (Fig. 2). The tool is a self-contained measurement device with its own software and data memory. It is used with the APC or XCB sampling tools. LAST-I is

[1] Hill, I.A., Taira, A., Firth, J.V., et al., 1993. *Proc. ODP, Sci. Results,* 131: College Station, TX (Ocean Drilling Program).
[2] Atlantic Geoscience Centre, Bedford Institute of Oceanography, Box 1006, Dartmouth, NS B2Y 4A2, Canada.
[3] The Christian Albrechts University of Kiel, Kiel, Federal Republic of Germany.
[4] University of Kiel, Kiel, Federal Republic of Germany.
[5] University of British Columbia, Vancouver, British Columbia, Canada.

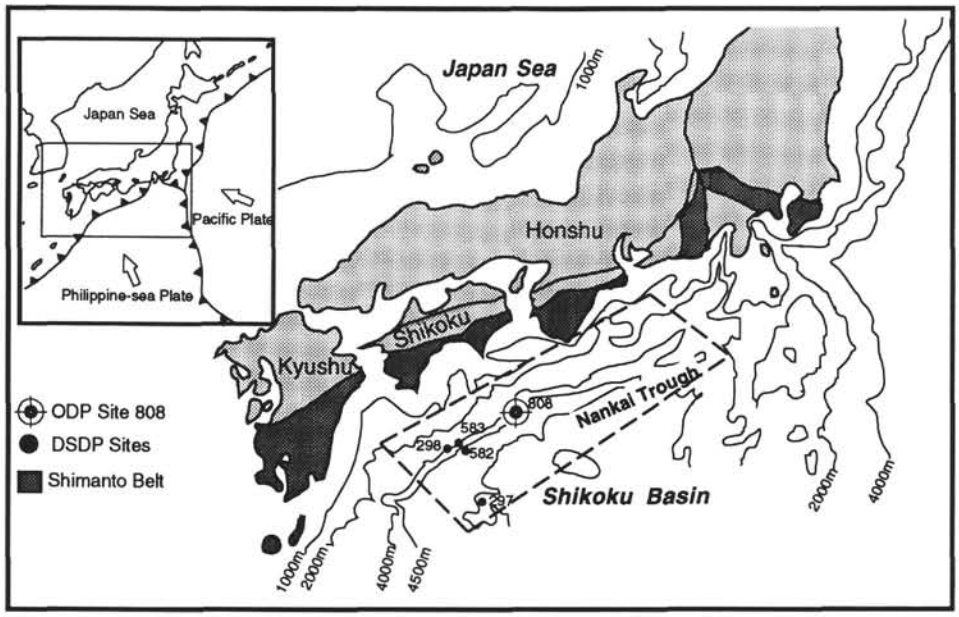

Figure 1. Regional map of the Nankai Trough showing the positions of DSDP and ODP drill sites.

pushed into the seabed formation ahead of the drill bit. After insertion into the formation, the tool is left for approximately 20 min while lateral stress and pore-pressure are measured and recorded. The tool measures effective lateral stress using three surface-mounted strain gauges positioned equally around the tool 120° apart and measures absolute pore-pressure using a strain-gauge-type pressure transducer (Fig. 2). The tool uses a reverse cutting shoe to minimize disturbance to sediment around the outer wall of the tool. The reverse cutting shoe was tested prior to ODP Leg 131 on a cruise to a basin on the Scotian Shelf offshore eastern Canada. These tests showed that in fine grained sediment, no plugging occurred within the sampling tube (Moran, 1988). A more detailed description has already been presented (Shipboard Scientific Party, 1991b).

RESULTS

Porosity-Depth Functions

Porosity (η) is the ratio of the volume of pore space to the total volume. In general, variations in η are controlled by lithologic changes downhole at Site 808 (Fig. 3). In the shallowest lithologies (slope apron and trench fill sediment), the porosity decreases overall with depth. However, large variations in porosity occur within these sedimentary facies. Porosity variations are largely a function of grain size within these lithologies which are represented by a wide range of interbedded gravity flows, specifically turbidites. Consequently, these two facies associations cannot be represented by a single porosity-depth function.

The frontal thrust at Nankai, Site 808 (Fig. 4), was intersected at approximately 365 mbsf. The sediment section from 365 to 410 mbsf is a repeated sequence of the thrusted sediment interval from 220 to 265 mbsf. Within this interval, laboratory porosity does not vary significantly with depth. Rather, the average porosity above and below the thrust varies from 51% to 44% in the lower axial trench wedge (LATW) facies and the average porosity (47%) does not statistically vary above and below the thrust in the outer marginal trench wedge (OMTW) facies (Fig. 3). The 7% porosity decrease with depth in the LATW facies can be attributed to its coarser grained sediment component and therefore more permeable behavior. The LATW facies likely experienced rapid drainage after this sediment sequence was vertically loaded by the overthrusted sediment. In contrast, because the average porosity above and below the thrust is the same for the OMTW facies, this lower permeability sediment has not yet had time to drain since the thrust event occurred, suggesting recent thrusting.

The OMTW facies association sediment, which lie below the thrust to a depth of 556.8 mbsf show no porosity reduction with depth (Fig. 3). Average porosity values at 409.5 mbsf and at the base of the facies association are the same at 45%. Sediments that are deposited as fine-grained turbidites and debris flows typically will display porosity functions that show only very small variations with depth because of large accumulation rates. The average sedimentation rate within this facies is very high, 1381 m/m.y. (Shipboard Scientific Party, 1991a). Under these depositional environments, high internal pore-pressures are easily generated as additional, thick sequences of sediment are loaded on top of previous rapidly deposited sediment packages.

The facies association trench-to-basin transition shows a relatively normal decrease in porosity with depth. Porosity decreases 4% over a depth interval of 62 m (Fig. 3). Below this transition, the Upper Shikoku Basin facies shows only a small decrease in average porosity with depth. The Lower Shikoku Basin sediments decrease in porosity with depth to 945 mbsf where the décollement was sampled. This facies decreases in porosity by 0.025% per meter, as approximated with a linear fitting function (Fig. 3). A change in the porosity-depth function occurs at the boundary between Upper and Lower Shikoku Basin sediment. In addition, scatter in porosity data decreases from the Upper to Lower facies, most likely due to a reduction in ash/tuff content in the Lower facies association.

At the décollement, a large porosity change occurs as a reduction. Porosity measured on core pieces sampled from the heavily fractured décollement is low and averages 28%, 5% lower than core samples measured in the core recovered just above. Given the highly fractured and sheared nature of the décollement, this reduction in porosity can be attributed to shear consolidation. These porosity values are lower than all others measured in the Shikoku Basin facies, even within deeper intervals, 300 m below the décollement.

The most dramatic change in porosity occurs just below the décollement where it anomalously and sharply increases to 37% (Fig. 3). This change in porosity is not associated with a lithologic boundary nor a diagenetic front, but likely represents a change in stress conditions

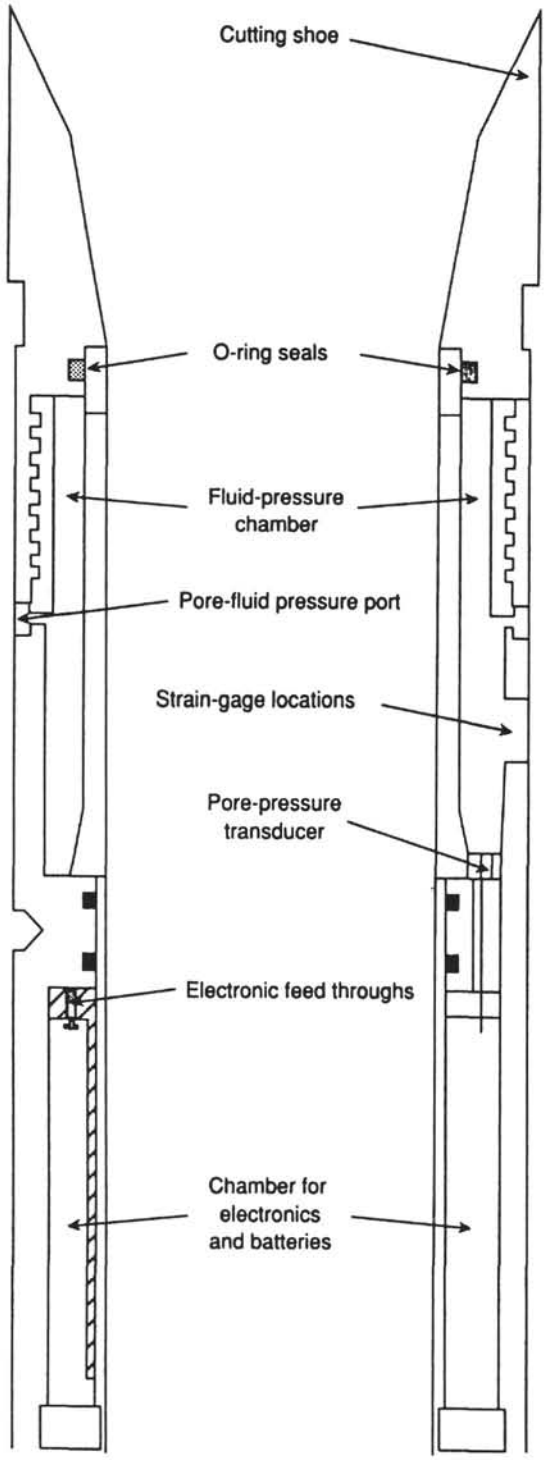

Figure 2. Schematic diagram of the phase I lateral stress tool (LAST-I). Note the reverse cutting shoe. The schematic depicts only one lateral stress sensor, but the tool has three sensors, positioned 120° apart in the same horizontal plane (Shipboard Scientific Party, 1991b).

across the décollement. However, below this porosity reversal, within the Shikoku Basin sedimentary facies, the porosity decreases once again normally with depth at a rate of 0.029% per meter.

Porosity decreases within the lower two facies, volcaniclastic deposits, and basalt as a result of compositional change. Although porosity decreases within the volcaniclastic unit with depth, this decrease is

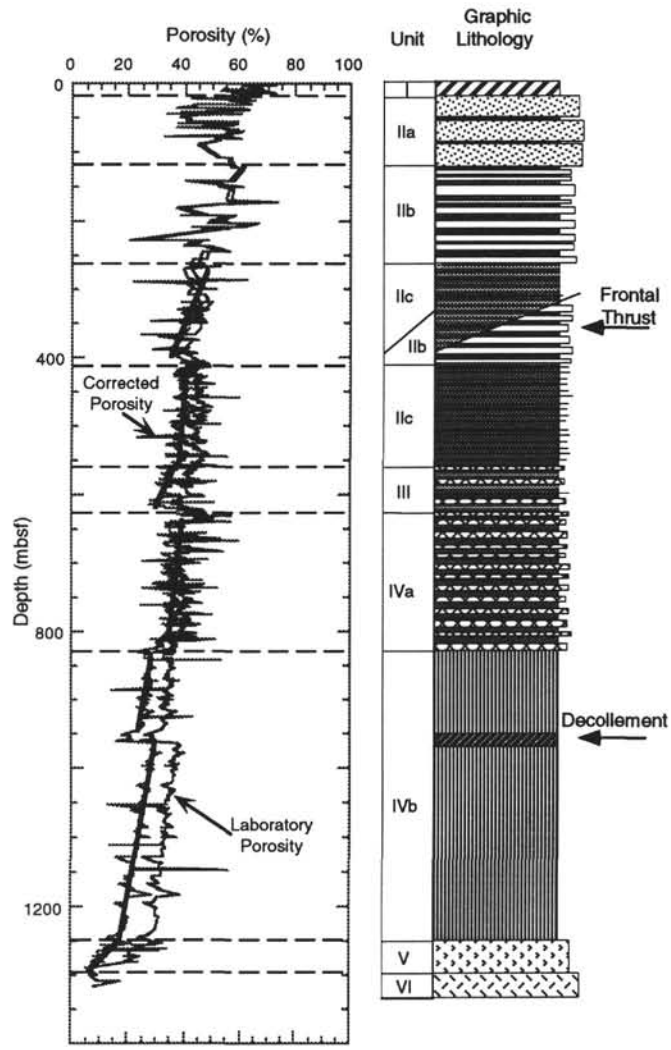

Figure 3. Porosity-depth relationships for Site 808 for each lithologic unit. The laboratory measured porosity is plotted together with porosity data that have been corrected for elastic rebound. The straight lines in the corrected porosity plot are linear-least squares curve fits to data within each lithologic unit. The upper three units (I, IIa, and IIb) show too much variability for straight line porosity-depth functions, due to the large dependence of porosity on grain size (modified from Shipboard Scientific Party, 1991a).

the result of an increase in basalt with depth and does not represent sediment consolidation.

One-Dimensional Consolidation Tests

One-dimensional consolidation tests were run on selected facies. Sediment, as it deforms during vertical consolidation, behaves both elastically and plastically. Sediment has a larger component of plastic or non-recoverable deformation than elastic or recoverable deformation. This rheological behavior led Casagrande (1932) to first interpret one-dimensional consolidation data in terms of sediment stress history. Casagrande showed that sediment retains a "memory" of its stress history. When a sample is loaded to a stress level that is greater than any of its previous in-situ stresses, the sediment sample will undergo significant additional plastic deformation. The laboratory sample is typically loaded one-dimensionally and allowed to drain or consolidate under incremental stress levels. The laboratory data are normally plotted as vertical effective stress vs. void ratio (Fig. 5),

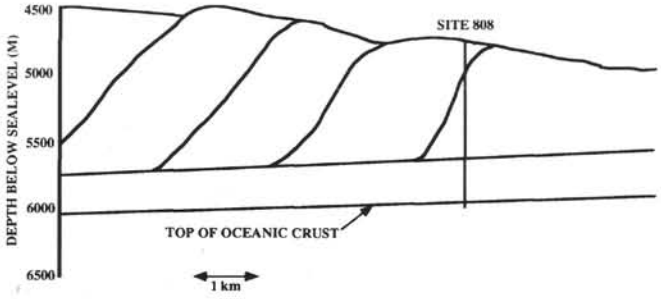

Figure 4. Simplified line drawing of some dominant high-amplitude reflections from seismic data collected in the vicinity of Site 808 (modified from Moore et al., 1991). The position and total length of the holes at Site 808 are also shown.

where void ratio (e) is defined as the ratio of the volume of pore spaces to the volume of the sediment grains and can be converted to porosity by: $\eta = e/(1 + e)$.

Consolidation test data have three major components: the reconsolidation curve, the virgin compression curve, and the rebound curve. The reconsolidation curve represents the sample's initial elastic response of the sediment upon reloading. The virgin compression curve represents the characteristic response (both plastic and elastic strain) of the sample response to effective stresses higher than the sample has been loaded to in-situ. The rebound curve is the elastic component of the total strain and can be used to define the amount of rebound experienced by the sediment as it is unloaded during sampling (see, e.g., Hamilton, 1976).

The maximum past pressure, also known as the pre-consolidation stress, is interpreted as the maximum past effective in-situ stress for conditions of one-dimensional strain (K_o). A sediment is interpreted as normally consolidated when the pre-consolidation stress (P_c') is equal to the existing vertical effective overburden stress (P_o'). A sediment is overconsolidated when the pre-consolidation stress is greater than P_o'. Underconsolidation exists when P_c' is apparently less than P_o'. Overconsolidation can occur, for example, when overburden is removed during erosional events, by ice sheets on the seafloor during past glaciations, and by diagenetic processes. Underconsolidation is a stress state wherein excess pore fluid pressures have not been dissipated and therefore inhibit the normal consolidation process. Underconsolidation can occur in environments of high sedimentation rates, in environments where additional loading of the seabed can occur, e.g., due to seafloor wave loading, where the rate of loading is high relative to sediment permeability. Thus, lower permeability sediment, which can restrict the dissipation of pore-pressure, is more susceptible to underconsolidation than highly permeable sediment. Excess pore fluid pressure does not necessarily define underconsolidated behavior because normal and overconsolidated sediment can also be subjected to excess fluid pressure. The overconsolidation ratio (OCR) is a non-dimensional parameter often used to classify the stress history of sediment. An OCR > 1 indicates overconsolidation, OCR < 1 underconsolidation, and OCR = 1 normal consolidation.

P_o' for Site 808 was calculated using the shipboard-measured bulk density data as follows:

$$P_o' = \Sigma\{(\rho - \rho_w)_i \times (z_i - z_{i-1}) \times g\}, \quad (1)$$

where at any depth increment (i), P_o' is determined using the shipboard measured bulk density (ρ), the density of the pore fluid (ρ_w), and the depth below seafloor (z). Site 808 shows a nearly linear increase with depth in P_c' with a deviation from this trend at the décollement (Fig. 6).

A total of seven tests were run on whole-round samples cut from XCB and RCB core samples from Holes 808B, 808C, and 808G (Table 1). The samples represent four different sediment types: lithofacies II, the Lower Axial Trench Wedge sediment; lithofacies IIc, the Outer Marginal Trench Wedge sediment; lithofacies IVa, Upper Shikoku Basin sediment; and lithofacies IVb, Lower Shikoku Basin sediment. In addition, the test on the sample from lithofacies IIc is positioned below the frontal thrust and is therefore likely affected by the additional stress loading of the thrusted sediment. The sample from lithofacies IVb is located below the décollement within the offscraped sediment package and is also likely influenced by additional vertical stresses caused by sediment loading during subduction.

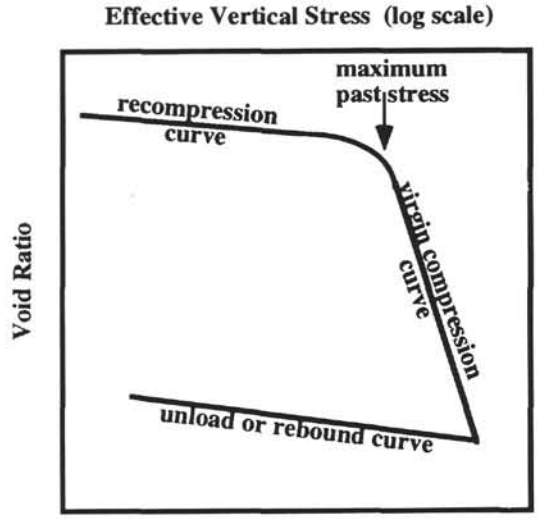

Figure 5. Typical one-dimensional consolidation test results plotted as effective stress vs. void ratio. The three components of the strain curve are labeled. Also shown is the maximum past pressure, which is determined by the maximum curvature between the reload and virgin compression portions of the curve.

For all tests, P_c' was determined following the Casagrande (1936) construction method. All samples except the shallowest are interpreted as under- to slightly overconsolidated (Table 1). The shallowest sample is slightly overconsolidated with an OCR = 1.5 (Fig. 7). Within the same lithofacies, two additional tests were run, which are interpreted as underconsolidated (OCR = 0.4). The average elastic rebound for this lithofacies is 2.8% void ratio per kPa. This rebound was applied to the laboratory porosity data to correct it to in-situ porosity (Fig. 3).

The sample from lithofacies IIc is interpreted as normally consolidated (Table 1 and Fig. 7). The rebound for this sediment type is very similar to lithofacies IIb. This rebound (6%/kPa) was applied to the entire unit's porosity data (Fig. 3). The Shikoku Basin facies tests suggest that the unit is underconsolidated and the sample from below the décollement (1034 mbsf) is severely underconsolidated with a P_c' of 260 kPa, equivalent to a normally consolidated sample of Shikoku Basin sediment located at a depth of 30 mbsf. The rebound of this unit ranges from 1.9% to 4.3%/kPa (Table 1). These rebound values were applied to the laboratory porosity data to determine the in-situ porosity (Fig. 3). The consolidation test results show underconsolidated behavior in the hemipelagic sediments above and below the décollement, suggesting excess pore fluid pressure and predominantly normally consolidated behavior elsewhere with some localized exceptions where the stress history is dominated by sedimentation rates.

LAST-I Results

LAST-I was deployed seven times in two holes, 808F and 808G. The first three deployments in Hole 808F were unsuccessful, primarily because the tool had never before been deployed on the *JOIDES Resolution*. However, these first three runs provided the operators with enough experience for successful deployments in Hole 808G. Although the remaining deployments were not all successful, three

Table 1. One-dimensional consolidation test data summary (preconsolidation stress could not be selected for the test at 671 mbsf).

Depth (mbsf)	Sample I.D.	Facies unit	Sediment rate (m/m.y.)	Preconsolidation stress (kPa)	Vertical effective stress (kPa)	OCR	Elastic rebound (% e/log kPa)
173	808B-7X-3	IIb	787	2000	1480	1.4	2.8
195	808G-8X-2	IIb	787	600	1608	0.4	2.8
199	808G-8X-4	IIb	787	1870	1690	1.1	2.8
514	808C-23R-3	IIc	1060	8000	4890	1.6	6
671	808C-39R-4	IVa	107	>1000	6490	>1.5	1.9
736	808C-43R-2	IVa	107	360	6831	0.1	1.9
1034	808C-77R-3	IVb	46	260	10011	0.0	4.3

of the last four tests recovered data. During Leg 131, the drill string experienced low frequency vibration due to the Kiroshio current. This vibration wreaked havoc on most of the downhole tools, and although LAST-I was not put out of commission, the tool was damaged. After the fourth deployment, one of the three lateral strain gauges was damaged beyond shipboard repair. Due to severe time constraints on Leg 131, deployments of LAST-I were relatively shallow at Site 808.

The tool measures two related parameters: pore-fluid pressure and lateral effective stress. The pore-pressure is measured directly using an absolute pressure transducer and the lateral stress is measured with a strain-gauged diaphragm that senses pore-pressure on one side and total lateral stress on the other side. In sediment, the total or lithostatic stress is related to effective stress by the effective stress principal (Terzaghi, 1943), the single most important concept in soil and rock mechanics. This concept is normally represented by:

$$\sigma_\tau = \sigma v' + u, \tag{2}$$

where σ_τ is the total normal stress, σ' is the effective normal stress, and u is excess pore-fluid pressure. The lateral stress tool measures σv in the horizontal plane as well as pore-fluid pressure. With these two measurements, the total normal stress state at any given depth can be determined because the vertical stress is determined from the bulk density of overburden (equation 1). The vertical effective stress as determined using equation 1 assumes hydostatic pore-pressure conditions. Therefore this determination must be corrected by subtracting any excess pore-fluid pressure above hydrostatic.

Two of the successful deployments recorded in-situ normal lateral stress, the first and third deployments in Hole 808G. These deployments are designated 808G-1 and 808G-3 and are positioned at 195.5 and 212.5 mbsf, respectively (Fig. 8). The records of lateral effective stress are direct measurements that show spikes during the initial placement of the tool and, for deployment 808G-3, also during pullout of the tool (Fig 8). These spikes are likely excess lateral stresses generated by movement of the tool relative to the formation. During the time period (approximately 20 min) when the tool was motionless in the hole, the record of lateral stress is constant for the two working sensors. This constant stress is interpreted as the effective lateral stress at each of these depths in the horizontal plane with sensors 2 and 3 positioned 120° apart (Table 2). The absolute orientation of these measurements was not measured. Stress ratios are commonly presented as values of lateral stress ratio (K), which is the ratio of effective horizontal to vertical normal stress. K_o is similar, but defined in terms of effective stresses. Normal vertically loaded sediments have K_o ratios of 0.4–0.5, reflecting a vertical major principal stress. The stress measurements at Site 808 result in K_o values ranging from 2 to 3 (Table 2), suggesting rotation of the principal stress direction to the horizontal. Total lateral stresses, based on these measurements range from 52.9 to 53.0 MPa.

All of the three successful deployments recorded pore-fluid pressure, designated 808G-1 (195.5 mbsf), 808G-3 (212.5 mbsf), and 808G-4 (222.5 mbsf). The pore fluid pressure response to insertion of the tool in the seafloor is normally an initially large increase followed by a decay to in-situ pressures. The increase is the result of the transfer of the insertion stress initially to the pore-fluid pressure. Decay of this initial "dynamic" excess pore-pressure is dependent upon sediment permeability. Highly permeable material will reach equilibrium pore-pressure rapidly, while low permeability material will take longer periods of time. Pore-pressure response from the LAST-I deployments show very high initial increases in pressure (>4 MPa) which rapidly decay to values interpreted as in-situ pore-pressure (Fig. 9). The in-situ pore-pressures for each deployment are in excess of hydrostatic fluid pressure. The in-situ pore-pressure was estimated for each deployment by a best fit to the pressure decay portion of the pore-pressure response (see Fig. 10, for example). Based on these curve fits, the excess fluid pressure for each deployment were determined and range from 320 to 385 kPa (Fig. 10 and Table 2).

In addition to direct measurement of pressure, the pore-pressure decay curve can be used to estimate in-situ permeability, in terms of the hydraulic conductivity. Pore pressure decay solutions around probes have been obtained by others (e.g., Levadoux and Baligh, 1986). These solutions express pore pressure decay as a function of the coefficient of consolidation. The coefficient of consolidation is proportional to the ratio of hydraulic conductivity to compressibility. Based on the solutions of pore pressure decay for different probe geometries and the relationship of the coefficient of consolidation with hydraulic conductivity (k), Baligh and Levadoux (1986) developed empirical functions for prediction of k in different sediment types from pore pressure data. This same method was applied in this study to the LAST-I pore pressure decay curves.

It was assumed that the LAST-I tool most closely approximates a narrow angle (18°) penetrometer. This approximation results in a

Table 2. LAST-I summary of test results, the calculated and corrected vertical effective stress, and the pore pressure parameter λ*.

Depth (mbsf)	Hydrostatic stress (kPa)	Vertical effective stress (kPa)	Corrected vertical effective stress (kPa)	Excess pore pressure (kPa)	Lateral stress 1 (kPa)	Lateral stress 2 (kPa)	K Range	λ*
186	49020	1564	1205	370	3187	2422	2.6–2.0	0.24
203	49191	1736	1378	320	3421	3218	2.5–2.3	0.18
213	49291	1838	1479	385				0.21

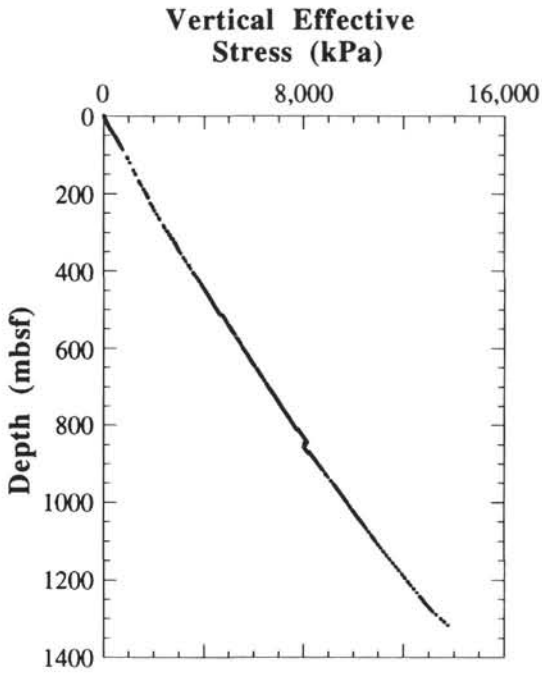

Figure 6. Vertical effective stress vs. depth below seafloor. The stress is calculated from laboratory measured bulk density data and assumes hydrostatic conditions.

small range of hydraulic conductivity for the three pore-pressure decay curves of 5.6×10^{-6} to 6.6×10^{-6} cm/s. These values are typical for silt-size sediment (Freeze and Cherry, 1979). These values of hydraulic conductivity are equivalent to permeability values on the order of 10^{-15} m^2.

DISCUSSION

Three data sets are used to describe the in-situ effective stress conditions at Site 808: laboratory porosity data, one-dimensional consolidation tests, and in-situ stress and pressure measurements. Consistencies and discrepancies in all three data sets are discussed, beginning with the deepest sediment in the section.

Beneath the décollement, the sediment porosity sharply increases to values that are much too high for their depth of burial, assuming normal consolidation. The one-dimensional consolidation test from below the décollement shows a severely underconsolidated sediment. The underconsolidation suggests that the sediment has excess fluid pressure which has inhibited the normal consolidation process where sediment porosity decreases through drainage of pore fluid. The severity of underconsolidation suggests very high excess fluid pressures and sediment that may be close to or very near failure. The porosity offset just below the décollement suggests that the sediment is not draining into the fault, normally considered a more permeable zone because of its highly fractured nature. Because the fault is likely more permeable than the surrounding sediment, the décollement must be inhibiting drainage of excess pore fluid pressure. Because low permeability is ruled out, the mechanism for inhibiting drainage must be higher pore-fluid pressure than the surrounding sediment units. If this is the case and the décollement is a high-pressure boundary, it follows that this boundary also acts to decouple shear stresses and does not allow any transfer of shear from above to below the boundary. In this setting, shear is represented by a rotation of principal stress, therefore, principal stresses are likely not rotated below the décollement. Given these constraints on stress, the cause of the excess pore-fluid pressure below the décollement can be attributed to one or a combination of three causes: (1) relatively rapid loading of overburden as these subducted sediments move deeper and deeper into the complex along the highly sheared décollement, (2) high sedimentation rates during original depositional processes, and (3) the additional vertical loading from the recently thrusted sediment section. Unfortunately, no in-situ stress data were collected at these depths at Site 808.

Above the décollement, within the Upper Shikoku Basin sediment, the consolidation test data again suggests underconsolidated behavior. This underconsolidation likely reflects excess pore-fluid pressure in the sediment. The absolute porosity-depth function for this unit is slightly higher than the Lower Shikoku Basin sediment, which is consistent with underconsolidation. This entire unit lies above the décollement and is therefore affected by rotation of principal stresses. This underconsolidated behavior can be attributed to one or a combination of three causes: (1) high sedimentation rates during original depositional processes, (2) additional vertical loading from the recently thrusted sediment section, and (3) higher than normal loading conditions with rotation of principal stresses.

Within the Outer Marginal Trench Wedge sediment, the consolidation test data reflect normally consolidated behavior. The porosity-depth function is not consistent with this interpretation, although this test is close to the Trench-to-Basin transition unit. The porosity-depth function in the transition unit is consistent with normally consolidated behavior. In addition, the sediment sampled in the consolidation apparatus may reflect normally consolidated behavior because of the highly sheared structure of this unit (Shipboard Scientific Party, 1991a). The shearing increases local permeability so that drainage of any excess fluid pressure can more easily occur.

Three consolidation tests were run in sediment above the frontal thrust within the Lower Axial Trench Wedge unit. The range of consolidation behavior is normal (shallowest test) to underconsolidation. There is no consistent porosity-depth function within this unit because the porosity is primarily a function of grain-size variations. Because of this dependence, the permeability of the sediment likely varies significantly from highly permeable sediment in the sand-dominated beds to lower permeability sediment in the silt to clay dominated beds. This variation in permeability is probably reflected in the variation in stress history from normally consolidated to underconsolidation. Close to the underconsolidated tests, in-situ LAST-I tests were run. The LAST-I data is consistent with rotation of principal stresses and suggests excess pore-fluid pressure. The excess pore-fluid pressure likely exists within this less permeable zone and has been dissipated in the zone of the shallowest consolidation test. The causes of the underconsolidation can be attributed to: (1) high sedimentation rates during original depositional processes, and (2) higher than normal loading conditions with rotation of principal stresses.

CONCLUSIONS AND RECOMMENDATIONS

The laboratory and in-situ physical property and stress measurements conducted at Site 808 suggest that the stress conditions are dominated by excess fluid pressures throughout the sediment section. In general, the porosity-depth functions reflect the stress history of the sediment column with relatively small decreases in porosity with depth, characteristic of underconsolidated behavior. For the first time, in-situ stresses were measured within a modern accretionary complex, confirming the rotation of principal stresses, even within the shallowest sediment units. The in-situ stress conditions at Site 808 can be summarized as follows:

1. Sediments above the frontal thrust are subjected to high lateral stresses or rotation of principal stresses.
2. Sediment above the décollement has excess fluid pressure, except in zones of higher permeability.
3. Below the décollement, the sediment is dominated by very high excess fluid pressure.
4. There is no rotation of principal stresses below the décollement.

These conclusions are based on a unique, but very limited data set. Further study of modern sediment wedges requires an order of magnitude increase in the number of in-situ and laboratory consolidation measurements to provide confidence in these stress interpretations.

REFERENCES*

Athy, L.F., 1930. Density, porosity and compaction of sedimentary rocks. *AAPG Bull.,* 14:1–24.

Baligh, M.M., and Levadoux, J.-N., 1986. Consolidation after undrained piezocone penetration. II: Interpretation. *J. Geotech. Eng. Div., Am. Soc. Civ. Eng.,* 112-7:727–745.

Bangs, N.L.B., Westbrook, G.K., Ladd, J.W., and Buhl, P., 1990. Seismic velocities from the Barbados Ridge complex: indicators of high pore fluid pressures in an accretionary complex. *J. Geophys. Res.,* 95:8767–8782.

Brückmann, W., 1989. Typische Kompakationsmuster mariner Sedimente and ihre Modifikation in einem rezenten Akkretionskeil (Barbados Ridge). *Beitr. Geol. Inst. Univ. Tübingen,* Rh. A, 5:1–135.

Casagrande, A., 1932. The structure of clay and its importance in foundation engineering. *In Contributions to Soil Mechanics 1925–1940.* Boston Soc. Civ. Eng., 72–113.

————, 1936. Determination of preconsolidation load and its practical significance. *Proc. 1st Conf. Soil Mech. and Found. Eng.* (Vol. 3). Am. Soc. Civ. Eng., 60–64.

Freeze, R.A., and Cherry, J.A., 1979. *Groundwater:* Englewood Cliffs, NJ (Prentice-Hall).

Hamilton, E.L., 1976. Variations of density and porosity with depth in deep-sea sediments. *J. Sediment. Petrol.,* 46:280–300.

Holtz, R.D., and Kovacs, W.D., 1981. *An Introduction to Geotechnical Engineering:* Englewood Cliffs, NJ (Prentice-Hall), 289.

Kaiko I Research Group, 1986. Taira, A., and Tokuyama, H. (Eds.), *Topography and Structure of Trenches Around Japan—Data Atlas of Franco-Japanese Kaiko Project, Phase I:* Tokyo (Univ. of Tokyo Press).

Langseth, M.G., and Moore, J.C., 1990. Introduction to special section on the role of fluids in sediment accretion, deformation, diagenisis, and metamorphism in subduction zones. *J. Geophys. Res.,* 95:8737–8742.

Levadoux, J.-N., and Baligh, M.M., 1986. Consolidation after undrained piezocone penetration. I: Prediction. *J. Geotech. Eng. Div., Am. Soc. Civ. Eng.,* 112:707–726.

Lowe, J., III, 1974. New concepts in consolidation and settlement analysis. *J. Geotech. Eng. Div., Am. Soc. Civ. Eng.,* 100:574–612.

Moore, G.F., Karig, D.E., Shipley, T.H., Taira, A., Stoffa, L., and Wood, W.T., 1991. Structural framework of the ODP Leg 131 area, Nankai Trough. *In* Taira, A., Hill, I., Firth, J.V., et al., *Proc. ODP, Init. Repts.,* 131: College Station, TX (Ocean Drilling Program), 15–20.

Moore, J.C., and Lundberg, N., 1986. Tectonic overview of Deep Sea Drilling Project transects of forearcs. *In* Moore, J.C. (Ed.), *Structural Fabrics in DSDP Cores From Forearcs.* Mem.—Geol. Soc. Am., 166:1–12.

Moran, K., 1988. Dawson 88048 Cruise Report. *Bedford Inst. of Oceanogr., Dartmouth.*

Shipboard Scientific Party, 1991a. Site 808. *In* Taira, A., Hill, I., Firth, J.V., et al., *Proc. ODP, Init. Repts.,* 131: College Station, TX (Ocean Drilling Program), 71–272.

————, 1991b. Special tools. *In* Taira, A., Hill, I., Firth, J.V., et al., *Proc. ODP, Init. Repts.,* 131: College Station, TX (Ocean Drilling Program), 61–70.

Terzaghi, K., 1943. *Theoretical Soil Mechanics:* New York (Wiley).

* Abbreviations for names of organizations and publications in ODP reference lists follow the style given in *Chemical Abstracts Service Source Index* (published by American Chemical Society).

Date of initial receipt: 6 January 1992
Date of acceptance: 14 October 1992
Ms 131SR-129

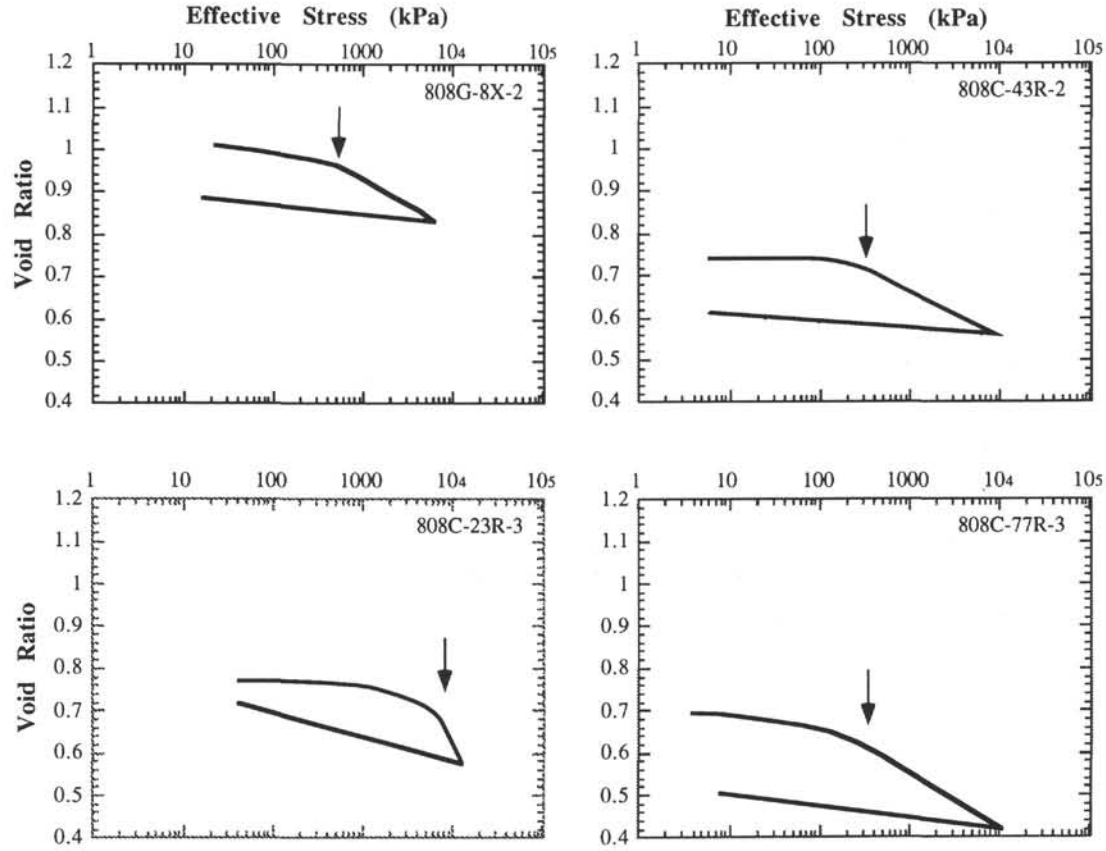

Figure 7. Effective vertical stress plotted on a log scale vs. void ratio for four of the seven consolidation tests, representing each lithofacies tested. The arrow in each plot denotes the interpreted preconsolidation stress or maximum past pressure.

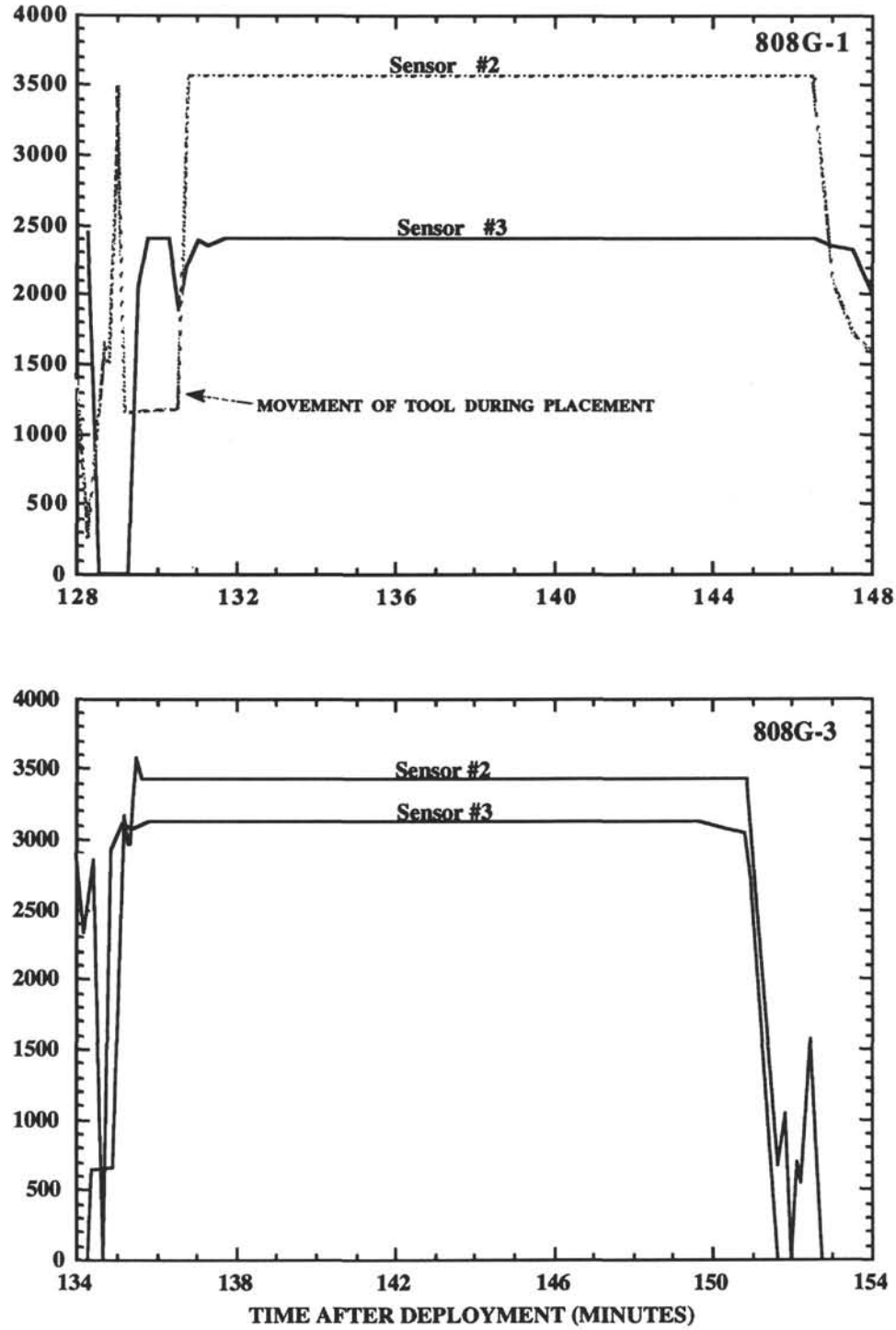

Figure 8. Lateral stress data from two deployments of LAST-I in Hole 808G.

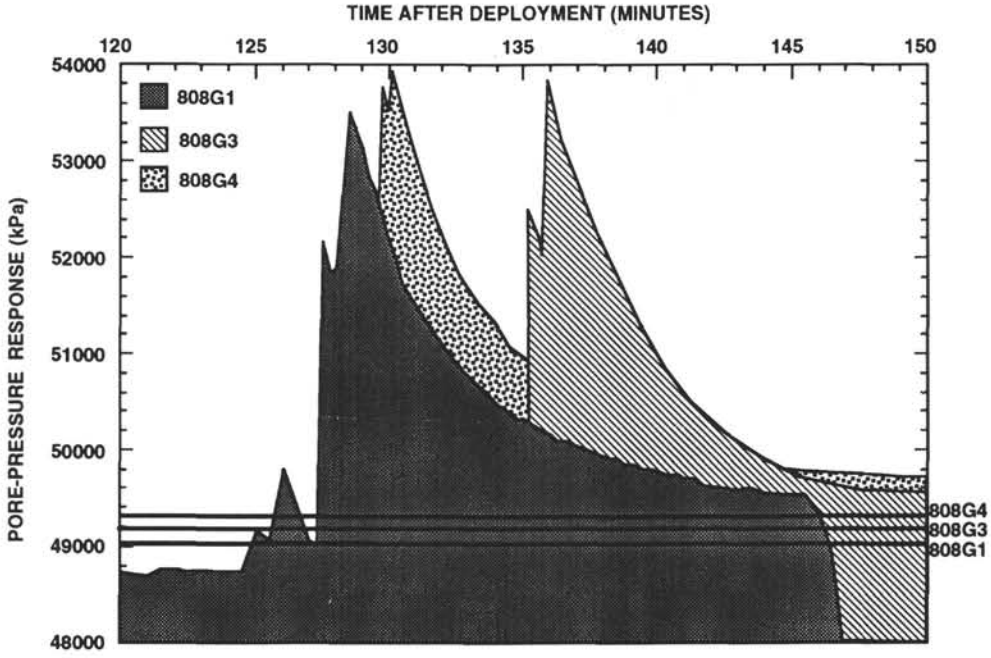

Figure 9. Pore-pressure response for three deployments of LAST-I in Hole 808G. The heavy lines represent the hydrostatic pore fluid pressure calculated for each depth of deployment. All decay curves are interpreted as representing excess fluid pressure.

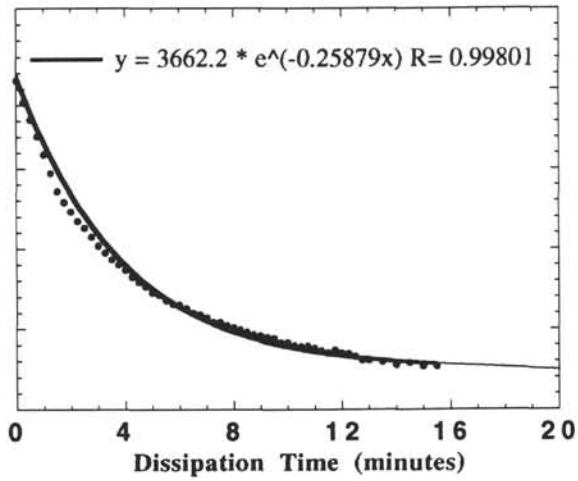

Figure 10. Exponential decay curve for the pore-pressure response data from LAST-I deployment 808G-1. This prediction results in an excess fluid pressure of 370 kPa for 808G-1. The vertical scale is 0 to 5000 kPa.